



ANALYSIS OF DYNAMOMETER SIGNALS OF INTERRUPTED CUTTING BY TIME-FREQUENCY LOCALIZATION METHODS

TAMÁS KOVÁCS

Kalmár Sándor Institute of Information Technology, Kecskemét College
6000 Kecskemét, Hungary
kovacs.tamas@gamf.kefo.hu

EDIT CSIZMÁS

Kalmár Sándor Institute of Information Technology, Kecskemét College
6000 Kecskemét, Hungary
csizmas.edit@gamf.kefo.hu

ANDRÁS SZABÓ

Institute of Metal and Polymer Processing Technology, Kecskemét College
6000 Kecskemét, Hungary
szabo.andras@gamf.kefo.hu

[Received November 2008 and accepted May 2009]

Abstract. In this work the force sensor signals of an interrupted metal cutting process were analyzed by continuous wavelets (CWT) and Hilbert-Huang Transformation (HHT). The main purpose was to characterize the signal through the typical behavior of its dominant frequencies and, at the same time, to compare the performances of the two frequency localizing methods applied. It was found that the low dominant frequencies are approximately constant while the values of the high dominant frequencies (above one kHz) show strong fluctuations. Here we show that the fluctuations revealed by the CWT method are caused partly by numeric effects of the method itself and partly by real variations in the frequency values. These variations are responsible for the non-stationary behavior of the signal. Regarding the methods applied, it was found that the wavelet analysis method is capable of tracing fast varying frequencies of the signal with values close to each other by the proper choice of the central frequency parameter of the mother wavelet. In comparison with the HHT, the wavelet method proved much more robust in this case.

Keywords: Continuous Wavelet Transform, Hilbert-Huang Transform, interrupted cutting

1. Introduction

The analysis of vibration signals is a useful method in research on cutting or other machining processes. A milling or a turning tool together with the

work-piece form a complex mechanical system containing different vibrating sub-systems, the frequencies of which carry relevant information about the whole system. Fourier and wavelet transforms, and recently the Hilbert-Huang Transform (HHT) are the main tools that can be applied in frequency determination. One of the the main motivations behind these examinations is the possibility of tool wear monitoring, diagnostics of tool breakage or other disfunctionalities of the machine. Application of wavelets can be found in various areas of machining processes. In most cases wavelet-based low-pass, high-pass or band filters are developed for signal processing or analyzing purposes. Sheffer and Heyns [1] applied wavelet decomposition of the force signal along with Fourier transform for tool condition monitoring. Li et al. [2] and later Bhattacharyya et al. [3] used wavelet spectrum coefficients for on-line monitoring of the tool wear state in turning and milling processes. Recently Shi and Gindy [4] proposed wavelets to decompose sensory signals into static and dynamic components and extract features of tool malfunctions in various machining processes. The possibilities of localizing varying frequencies in the signal were investigated theoretically in details by Delprat et al. [5] and Torr sani [6].

The other motivation in the force signal analysis is related to the area of active vibration control by a sensor-actuator system. Recently El-Sinawi and Kashani [15] and later Al-Zaharnah [16] designed and implemented such a control system by magnetostrictive actuators in the case of interrupted cutting. Their system does not use any a priori information about the frequencies or other characteristics of the vibration sources. If we had this information or at least part of it, the performance of such a control system could be improved by involving stochastic prediction of the vibration to be damped.

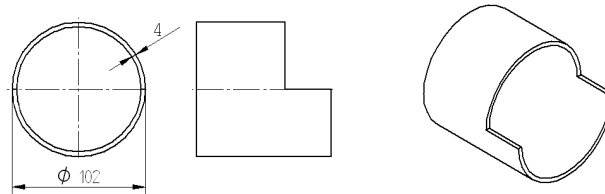


Figure 1. The truncated tube as work-piece

In this work the feed-force signal of an orthogonal interrupted cutting process is studied. In such processes the cutting tool collides with the work-piece with a certain frequency, and this launches the vibration modes of the sub-systems of the whole machine. In addition to this, in the continuous cutting phase

(between the entry and the exit of the cutting insert) there are various physical effects that similarly excite the vibration modes though with much smaller energy. Because of these impulse-like or continuous excitations the force sensor signal contains the frequencies of the activated vibration modes. Here we propose a Continuous Wavelet Transform (CWT)-based analysis of the vibrating force signals that is capable of tracing the fast varying frequencies of the different sub-systems, and, at the same time, it seems to be robust enough. A Hilbert-Huang Transform-based analysis of the signal is also performed in order to compare the two relevant methods.

2. Experimental

In the experimental part an orthogonal cutting arrangement was set by turning the free end of a structural steel tube, the end of which was truncated as shown in Fig. 1. The external diameter and the wall thickness of the tube was 102 mm and 4 mm, respectively. The machine applied was a general purpose double engine (2x5.5 kW) lathe equipped with T25M coated cemented carbide inserts. The geometry of the insert is characterized by a rake angle 5° and inclination angle 0° . The feed rate was 0.1 mm per revolution, and the rotations per minute (RPM) of the machine was 270. The applied cutting speed was calculated as

$$v = \pi Dn, \quad (2.1)$$

where D is the diameter of the tube and n is the RPM value. By means of Equation (2.1) the value of v was approximately 85 m/min. The magnitude of the force components was measured by a Kistler dynamometer, which was connected to a PCI National Instruments data acquisition card. The sampling frequency of the dynamometer was very high (200kHz) in order to get a good resolution of the force signal. The data were processed by LabView 7.1 software. In Fig. 2 the signal produced by the feed force can be seen.

3. Stationarity of the signal

As mentioned above, the analysis of the force signal is important for inventing proper stochastic prediction methods, which can help the vibration control system. The aim of these methods could be summarized as predicting the signal value a certain time in advance. In the present area this time should be a few tenths of milliseconds, since the reaction times of the magnetostrictive or piezoelectric actuators are in this order of magnitude. In the case of stochastic signals the most common technique is the linear prediction method [13]. This

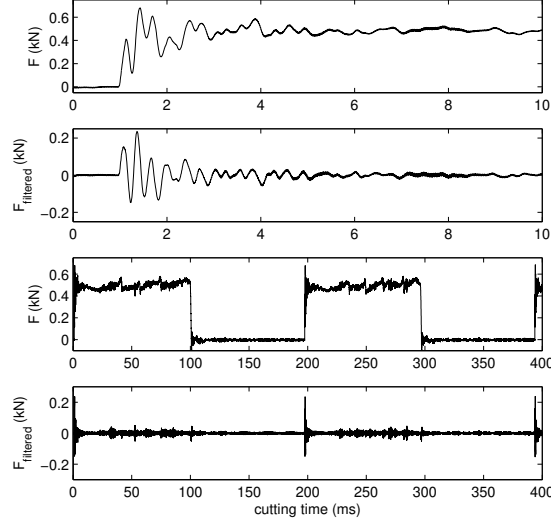


Figure 2. The original and the filtered (see eq. (3.3)) feed force signal measured in the first 10 and 400 milliseconds (two whole turning cycles) at the cutting speed 85 m/min and feed ratio 0.1 mm/rev. The zero of the time axis is taken to be one millisecond before the first workpiece-tool impact.

method assumes that the signal is at least weakly stationary. Among others, the weak stationarity demands that the signal's autocorrelation, defined by

$$X(t, L) = \langle F(t)F(t + L) \rangle, \quad (3.1)$$

is independent of time t and depends on only the time lag L . In the definition above $F(t)$ denotes the time dependent signal and the brackets $\langle \rangle$ stand for the normalized mean value. In order to characterize the weak stationarity of $F(t)$ we calculate the approximate value of the autocorrelation inside any time interval of length T , where T is large enough to get a reliable approximation. In mathematical terms, we determine the function defined by

$$X_T(t, L) = \langle F(t)F(t + L) \rangle_{[t-T/2, t+T/2]} = \frac{\int_{t-T/2}^{t+T/2} F(t)F(t + L)dt}{\int_{t-T/2}^{t+T/2} (F(t))^2 dt}. \quad (3.2)$$

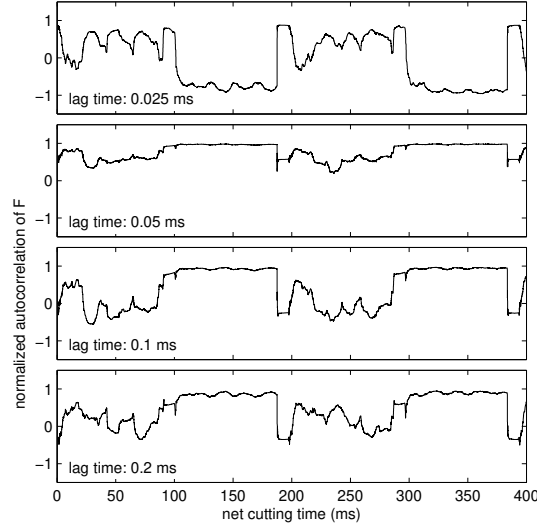


Figure 3. The autocorrelation function of the feed force signal at cutting speed 85 m/min and feed 0.1 mm/rev measured during the first 400 milliseconds (two whole turning cycles) for four different values of the time lag. The time periods of the free running can be seen as relatively constant plateaus in the autocorrelation graph.

By means of the condition mentioned, if the signal is weakly stationary then $X_T(t, L)$ should be a constant function with respect to variable t at any fixed value of L . Since we are interested in only the high frequency component of the signal (in the order of 1 kHz), first the low frequency part is removed from the signal by subtracting its sliding window average, that is

$$F_{filtered}(t) = F(t) - \frac{1}{W} \int_{t-W/2}^{t+W/2} F(\tau) d\tau, \quad (3.3)$$

where the length of the averaging time window (W) was chosen to be 0.1 milliseconds. The function $X_T(t, L)$ was calculated with the filtered feed force signal of six consecutive turning cycles, which means about 600 milliseconds net cutting time (i.e. omitting the free running time intervals), for the fixed values of time lag L of 0.025, 0.05, 0.1 and 0.2 milliseconds. The length of time segment T was chosen to be 10 milliseconds. The resulting four autocorrelation functions (for the four different lag times) can be seen in Fig. 3. The time segments of the free running of the tool were cut out from the signal. Since the reaction times of the piezoelectric or magnetostrictive actuators are a few tenth

of milliseconds, the last two graphs are the most interesting when $L = 0.1$ and 0.2 milliseconds. It can be seen that the graphed autocorrelation functions are far from being constant at any values of the time lag, so the signal should be considered non-stationary. In the case of the smallest lag ($L = 0.025$) there are periodic sharp deflections at the transient phases when the tool collides with the workpiece, but the fluctuations in other time intervals are also remarkable though not so outstanding as in the transient phase. For higher time lags the fluctuations became so intensive that the periodic deflections of the transient phase cannot be observed. These results indicate that the linear predictive methods with constant coefficients cannot be applied successfully for such cutting force signals, moreover, because of the fast variation of the autocorrelation value it is difficult to find even a time dependent adaptive linear prediction method. What are the basic reasons of such a bad non-stationary behavior of the signal? Since the normalized autocorrelation is more or less independent of the variations of the amplitude [14], the answer should be searched for in the variations of the dominant frequencies in the high frequency domain.

4. The tools of the frequency analysis

For accomplishing the wavelet analysis of the signal the symmetric Morlet function was chosen as mother wavelet, defined by

$$\phi(t) = \frac{1}{\sqrt{2\pi}} \exp\left(-\frac{1}{2}t^2 + i\omega_0 t\right). \quad (4.1)$$

The mother wavelet is scaled by a parameter a so as to get a characteristic frequency ω_0/a , and it is shifted in the time domain by a parameter b . Thus a set of wavelets (child wavelets) with different frequencies and time-positions is obtained as follows

$$\phi_{a,b}(t) = \frac{1}{\sqrt{2\pi a}} \exp\left[-\frac{1}{2}\left(\frac{t-b}{a}\right)^2 + i\omega_0\left(\frac{t-b}{a}\right)\right]. \quad (4.2)$$

The coefficients of the CWT are obtained by calculating the convolution integral:

$$\hat{F}(a,b) = \int_0^\infty \phi_{a,b}^*(t) (F(t) + iH[F(t)]) dt, \quad (4.3)$$

where $H[F(t)]$ is the Hilbert transform of the signal and $*$ stands for the complex conjugation. The expression $F(t) + iH[F(t)]$ is generally addressed as the

analytical form of $F(t)$. The most simple way of determining the dominant modes in the frequency and time scale is to find the local maximum places of $|\hat{F}(a, b)|^2$, which is regarded as the energy density function of the vibration [5],[6],[7]. The choice of the parameter ω_0 in the mother wavelet is crucial in the present task. This parameter determines the number of observable periods in the mother and also in the child wavelets. It can be easily seen that for bigger values of ω_0 (many periods in the wavelet) the selectivity of the wavelets in the frequency domain is better, i.e., the $\delta\omega$ error of frequency localization is smaller but the δt error of that in the time domain is bigger, and the contrary case is true when we choose a small value of ω_0 (few periods in the wavelet). Unfortunately, the two errors cannot be small at the same time, similarly to Heisenberg's law in quantum mechanics. In this work the $\hat{F}(a, b)$ spectra were calculated with more different (small and big) parameter values so as to get good resolution in the time and frequency domain, though not at the same time.

The HHT is based on completely different theoretical methods. In the first phase the so-called Empirical Mode Decomposition (EMD) decomposes the signal into approximately monochromatic, though possibly frequency and amplitude modulated components [8]. Then the instant frequencies are obtained by derivating the phase (argument) of the analytical components with respect to time, that is

$$\omega_k(t) = \frac{d}{dt} \arg (C_k(t) + iH[C_k(t)]), \quad (4.4)$$

where $C_k(t)$ is the k th component. There are a number of improvements of the original algorithm, especially regarding the EMD [9],[10],[11]. Here we apply the algorithm recently proposed by Rilling et al. [10]. The HHT, being a differential method, is able to give the instant frequency at a specific point of the time-scale, while the "instant" frequency obtained by CWT is localized in a finite time interval, which the envelope of wavelet spans over. However, a serious drawback of this method is that the EMD is of limited capability when components with frequencies close to each other are to be decomposed [8],[14].

5. Results and discussion

The results of the CWT and HHT analysis of the signal in Fig. 2 are presented here. The Fourier Transform of the signal measured during a complete turning cycle (approximately 80 ms) is seen in Fig. 4. There are four dominant

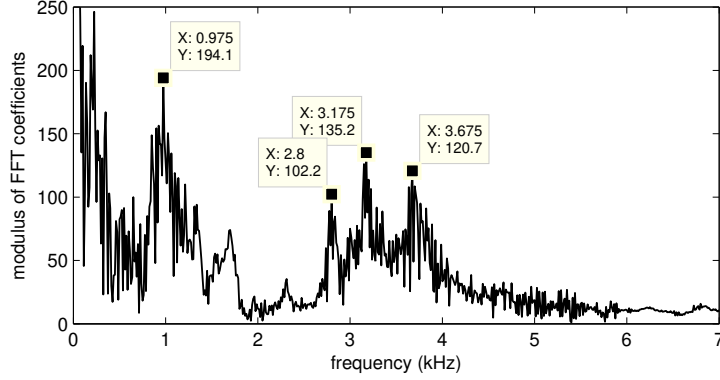


Figure 4. Fourier Transform of the analytical form of the feed force signal at cutting speed 85 m/min and feed 0.1 mm/rev measured during a complete turning cycle (80 milliseconds)

peaks in the region of higher frequencies at $f_1 = 1.0$, $f_2 = 2.8$, $f_3 = 3.2$ and $f_4 = 3.7$ kHz, where the frequency f is related to the angular frequency ω as $f = \omega/(2\pi)$. The latter three values are relatively close to each other, all of them being in the band of 2.5–4 kHz. Separating frequencies with values close to each other is a hard task for any known time-frequency localization methods [8]. In the case of a signal that consists of several components with frequency values constant but close to each other the CWT, because of the imperfect resolution in the frequency domain, leads to more or less fluctuating time-frequency functions. Therefore, in the case of the present force signal we should expect some fluctuations in the frequency values, which is not 'real' but a purely numeric effect.

In order to get a qualitative picture about this kind of numeric effect, an $F_{test}(t)$ test signal is constructed as a sum of three harmonic signals with the constant frequencies f_1 , f_2 , f_3 and f_4 , and the ratios between their amplitudes are chosen to be the same as those of the FFT coefficients in Fig. 4, i.e.

$$F_{test}(t) = \sum_{i=1,2,3,4} a_i \cos(2\pi f_i t), \quad (5.1)$$

where $a_1 = 1.9$, $a_2 = 1.0$, $a_3 = 1.4$ and $a_4 = 1.2$. This signal belongs to a dynamic system of four undamped harmonic subsystems without coupling. Fig. 5 shows the results obtained by applying the CWT-based method detailed in the previous section on the test signal with the ω_0 values of 10, 15, 20 and 25. The CWT results are generally given by a level curve or color-coded graph of

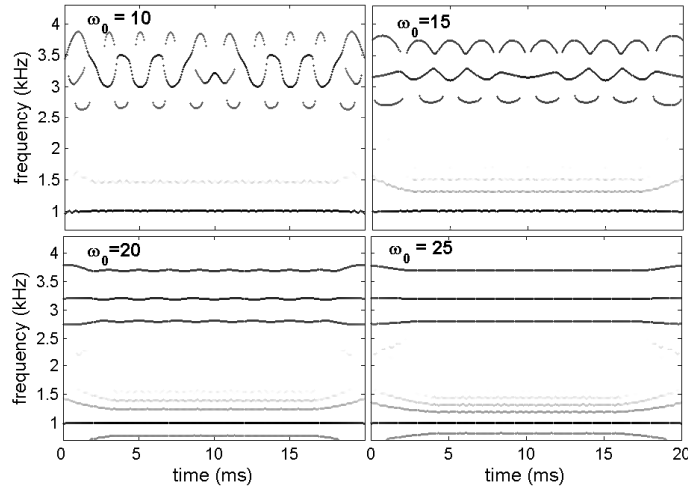


Figure 5. Local maximum places (at each fixed time value) of the energy density function obtained by CWT of the test signal given by (5.1) for four different values of ω_0 . The tone of the marker specs is linearly proportional to the logarithm of the local energy density.

the energy density function $|\hat{F}(a, b)|^2$. In the present work, however, only the places of the local maxima belonging to a fixed value of time are plotted in the time-frequency plane indicating the energy density at the local maxima by the darkness of the marker. To be more specific, the tones of the marker specs are linearly proportional to the logarithm of the local energy density, the highest and the lowest energy peaks corresponding to pitch black and white tones. Though this way of the presentation carries poorer information compared to the conventional ones, it gives a clearer picture about the behavior of the dominant frequencies. The fluctuations of the frequency values in these graphs are obviously caused by the numeric effect described above. However, these numeric fluctuations almost vanish when the value of the ω_0 parameter is increased to 20, and there is no considerable change for the further increase of ω_0 . Therefore, for the value of 20 of ω_0 the resolution is satisfactory in separating the present dominant frequency values with the measured ratios of the amplitudes. However, the case is different for the lowest frequency component. Since it is far enough from the other three in the frequency scale, its frequency is measured to be approximately constant even for the smallest value of ω_0 . Besides, false components appear for any values of ω_0 above the frequency f_1 , which is due to an aliasing effect. The higher ω_0 is, the more pronounced this effect is.

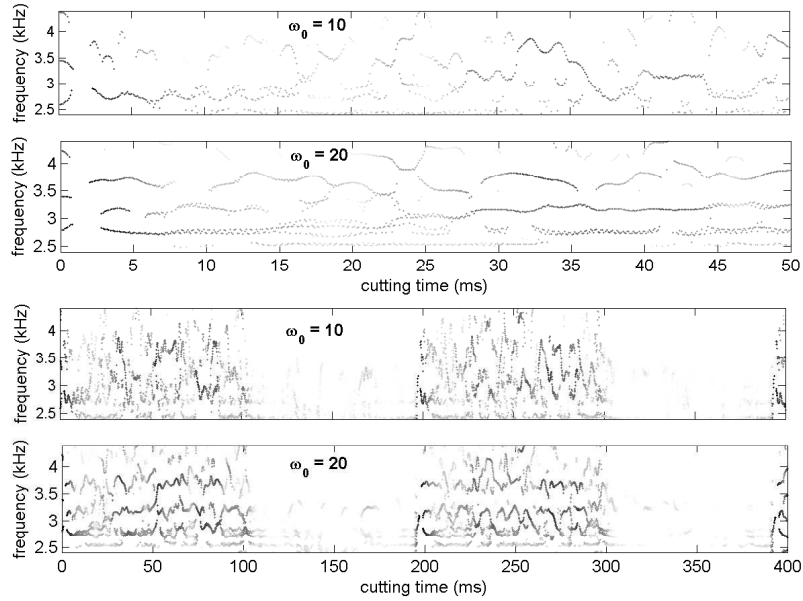


Figure 6. Local maximum places (at each fixed time value) of the energy density function obtained by CWT of the measured signal in the first 10 and 400 milliseconds for two different values of ω_0 . The chosen frequency region in the present case was 2.5-4.5 kHz. The tone of the marker specs is linearly proportional to the logarithm of the local energy density.

The feed force signal investigated was subject to the same CWT calculations with values of 10 and 20 of the self frequency parameter ω_0 . Fig. 6 and Fig. 7 show the results of the calculations for the higher and lower frequency regions. The figures were constructed by the same method as that applied in the case of Fig. 5. By means of experiences learned from the CWT of the test signal, the graphs of $\omega_0 = 10$ are contaminated by numerical fluctuations if there are frequency values close to each other, and, in addition to this, there can be 'real' variations of the frequency values. Nevertheless, the numeric fluctuations almost vanish when the ω_0 self frequency parameter is increased to 20. In the figure of the lower frequency region (Fig. 7) we can discover the dominant frequency of $f_1 = 1.0$ kHz together with false aliasing frequencies. There are no serious fluctuations of any kind, which means that there are no real dominant frequencies close to f_1 , and this component of the signal has approximately constant frequency. Regarding the higher frequency region the case is completely different: there are large fluctuations of the three dominant frequency values for both cases of $\omega_0 = 10$ and $\omega_0 = 20$. The false (only

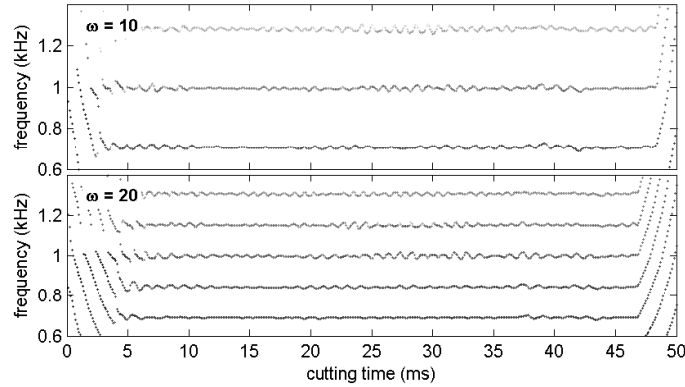


Figure 7. Local maximum places (at each fixed time value) of the energy density function obtained by CWT of the measured signal for two different values of ω_0 in the frequency region 0.6-1.4 kHz. The tone of the marker specs is linearly proportional to the logarithm of the local energy density.

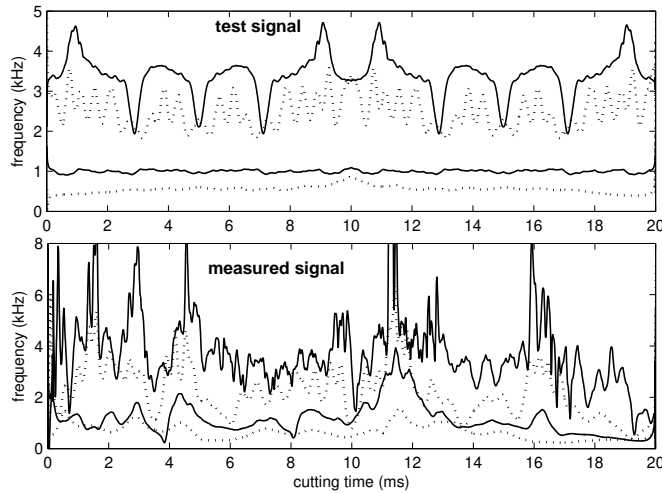


Figure 8. Frequencies of the four relevant components in the first 20 millisecond segment of the test and the measured signals obtained by HHT (continuous and dashed lines)

numeric) fluctuations were expected for $\omega_0 = 10$ because of the frequency values being relatively close to each other, however, when $\omega_0 = 20$ there are still serious fluctuations. This means that the vibration modes in the upper frequency region have physically varying frequencies. This real variation in

the frequency values can cause the non-stationary behavior of the force signal. It is also interesting that the energy seems to flow between the main vibration modes (remember, the black line segments are the high energy parts). This indicates that there are couplings between the three vibration modes. This can be one of the causes of the frequency modulations. Obviously, there may be other non-linear physical phenomena behind the frequency modulations as well. The investigation of the specific physical causes is beyond the scope of this paper.

For the sake of the comparison of the two relevant methods the HHT transform of the test and the measured signal at hand were calculated as well. The algorithm published electronically as a MATLAB package by Rilling et al. [10] was used here with stopping error limits ten times smaller than the default values set in the program package. Fig. 8 shows the time-frequency functions of the four components obtained by the HHT in the frequency region above 1 kHz. The fluctuations of the frequencies given by this method are much higher, which is partly due to the high precision local property of the HHT. In other words, this method is much more sensitive to the different kinds of noises and therefore seems to be much less robust than the CWT. It is to be noted that the HHT method does not give constant frequency-time functions even for the constant frequencies of the test signal (upper figure). Recently Rilling and Flandrin [12] investigated the theoretical limitations of EMD and they found that this method in its present form cannot separate two harmonic signals if the frequencies are close to each other or the lower frequency component has a considerably bigger amplitude than the higher one. This is the other reason for the wide fluctuations of the frequency values detected by the HHT. In the case of the test signal the two lower frequencies are distinguishable while the upper two are not. The reason for this is that the upper two frequencies are relatively too close to each other to apply the EMD method successfully (for a quantitative analysis see [12]). In addition to this, in the graph corresponding to the measured signal it is impossible to discover the dominant separate frequency peaks observed in the FFT graph, while the CWT method can identify these dominant frequencies.

6. Conclusions

The measured interrupted cutting force signal proved to be non-stationary with relatively fast varying autocorrelation, and this can be a serious drawback in the stochastic prediction of the signal. The CWT examinations showed that non-stationarity is caused by the considerable frequency modulations of the vibration modes in the frequency region above 2 kHz. An effective prediction

of the signal in this frequency region can be successful only if the physical reasons of the frequency fluctuations are analyzed in details. The CWT method proposed in the present work can be a helpful tool for such a physical analysis, since with its help the time evolution of the main frequency values and the energy content of the different modes can be monitored effectively. Naturally, to obtain a complete picture about the dynamics of the system, other types (acoustic and accelerometer) of measurements are also needed. This is left to a future work.

From the point of view of the numerical methods the results led us to the conclusion that the CWT should remain an important tool in time-frequency analysis problems, especially when the signal contains frequency and amplitude modulated vibrations in a relatively narrow frequency band. Besides, calculating the wavelet spectrograms for higher values of the self frequency parameter (ω_0) of the mother wavelet proved to be useful in separating real (physical) frequency variations from numeric fluctuations.

Acknowledgements

The support provided by the Annual Research Foundation of the Kecskemét College is acknowledged. We would like to thank Norbert Földvári for his help in editing our figures.

REFERENCES

- [1] SHEFFER, C., HEYNS, P. S.: *Wear monitoring in turning operations using vibration and strain measurements*, Mechanical Systems and Signal Processing, **15/6**, (2001), 1185–1202.
- [2] LI, X., GUAN, X. P.: *Time-frequency analysis-based minor cutting edge fracture detection during end milling*, Mechanical Systems and Signal Processing, **18**, (2004), 1485–1496.
- [3] BHATTACHARYYA, P., SENGUPTA, D., MUKHOPADHYAY, S.: *Cutting force-based real-time estimation of tool wear in face milling using a combination of signal processing techniques*, Mechanical Systems and Signal Processing, **21**, (2007), 2665–2683.
- [4] SHI, D., GINDY, N. N.: *Development of an online machining process monitoring system: Application in hard turning*, Sensors and Actuators A, **135**, (2007), 405–414.
- [5] DELPRAT, N., ESCUDIÉ, B., GUILLEMAIN, P., KRONLAND-MARTINET, R., TCHAMITCHIAN, PH., TORRÉSANI, B.: *Asymptotic Wavelet and Gabor Analysis: Extraction of Instantaneous Frequencies*, IEEE Trans. Inf. Th., **38**, (1992), 644–664.

-
- [6] TORRÉSANI, B.: *Time-Frequency analysis from geometry to signal processing*, Proceedings of the COPROMATH conference (November 1999, Cotonou, Benin), J. Govaerts, N. Hounkonnou and W. A. Lester Eds., World Scientific, (2000), 74–96.
- [7] CARMONA, R., HWANG, W. L., TORRÉSANI, B.: *Characterization of Signals by the Ridges of their Wavelet Transform*, IEEE Trans. Signal Processing, **45/10**, (1997), 2586–2590.
- [8] HUANG, N. E., SHEN, Z., LONG, S. R., WU, M. C., SHIH, H. H., ZHENG, Q., YEN, N., TUNG, C. C., LIU, H. H.: *The empirical mode decomposition and the Hilbert Spectrum for nonlinear and non-stationary time series analysis*, Proc. R. Soc. Lond. A, **454**, (1998), 903–995.
- [9] PENG, Z. K., TSE, P. W., CHU, F. L. : *An improved Hilbert-Huang transform and its application in vibration signal analysis*, J. Sound and Vibration, **286**, (2005), 187–205.
- [10] RILLING, G., FLANDRIN, P., GONCALVES, P.: *On Empirical Mode Decomposition and its algorithms*, IEEE-EURASIP Workshop on Nonlinear Signal and Image Processing NSIP-03, Grado (I), (2003).
- [11] YINFENG, D., YINGMIN, L., MINGKUI, X., MING, L.: *Analysis of earthquake ground motions using an improved Hilbert-Huang transform*, Soil Dynamics and Earthquake Engineering, **28**, (2008) 7–19.
- [12] RILLING, G., FLANDRIN, P.: *One or Two Frequencies? The Empirical Mode Decomposition Answers*, IEEE Trans. Signal Processing, **56/1**, (2008), 85–95.
- [13] HAYES, M. H.: *Statistical Digital Signal Processing and Modeling*. , J. Wiley & Sons, Inc., New York, (1996).
- [14] RUBIO, E. M., TETI, R., BACIU, I. L.: *Advanced Signal Processing in Acoustic Emission Monitoring for Machining Technology*, Intelligent Production Machines and Systems, Ed. by D.T.Pham, E.E.Eldukhri and A.J.Soroka, Elsevier Ltd., Cardiff, UK, (2006).
- [15] EL-SINAWI, A. H. AND KASHANI, R.: *Improving Surface Roughness in Turning Using Optimal Control of Tool's Radial Position*, J. Materials Processing Technology, **167**, (2005), 54–61.
- [16] AL-ZAHARNAH, I. T.: *Suppressing Vibrations of Machining Processes in Both Feed and Radial Directions Using an Optimal Control Strategy: The Case of Interrupted Cutting*, J. Materials Processing Technology, **172**, (2006), 305–310.